Site occupancy, magnetic moments, and elastic constants of off-stoichiometric Ni_2MnGa from first-principles calculations

Qing-Miao Hu*
Shenyang National Laboratory for Materials Science, Institute of Metal Research, Chinese Academy of Sciences, 72 Wenhua Road, Shenyang 110016, China and Department of Materials Science and Engineering, Applied Materials Physics, Royal Institute of Technology, Stockholm SE-100 44, Sweden

Chun-Mei Li and Rui Yang
Shenyang National Laboratory for Materials Science, Institute of Metal Research, Chinese Academy of Sciences, 72 Wenhua Road, Shenyang 110016, China

Svetlana E. Kulkova
Institute of Strength Physics and Materials Science, Siberian Branch of Russian Academy of Science, 2/4 Akademichesky, Tomsk 634021, Russia

Dmitry I. Bazhanov
Faculty of Physics, Moscow State University, 1-2 Lenin Hills, Moscow 119992, Russia

Börje Johansson
Department of Materials Science and Engineering, Applied Materials Physics, Royal Institute of Technology, Stockholm SE-100 44, Sweden; Department of Physics, Condensed Matter Theory Group, Uppsala University, Uppsala SE-75121, Sweden; and School of Physics and Optoelectronic Technology and College of Advanced Science and Technology, Dalian University of Technology, Dalian 116024, China

Levente Vitos
Department of Materials Science and Engineering, Applied Materials Physics, Royal Institute of Technology, Stockholm SE-100 44, Sweden; Department of Physics, Condensed Matter Theory Group, Uppsala University, Uppsala SE-75121, Sweden; and Research Institute for Solid State Physics and Optics, Budapest H-1525, P.O. Box 49, Hungary
(Received 5 February 2009; revised manuscript received 15 March 2009; published 10 April 2009)

The site occupancy and elastic modulus of off-stoichiometric Ni_2MnGa alloys are investigated by the use of the first-principles exact muffin-tin orbital method in combination with coherent-potential approximation. The stable site occupancy at 300 K is determined by comparing the free energies of the alloys with different site-occupation configurations. It is shown that, for most of the off-stoichiometric Ni_2MnGa, the "normal" site occupation is favorable, i.e., the excess atoms of the rich component occupy the sublattice(s) of the deficient one(s). Nevertheless, for the Ga-rich alloys, the excess Ga atoms have strong tendency to take the Mn sublattice no matter if Mn is deficient or not. Based on the determined site occupancy, the elastic moduli of the off-stoichiometric Ni_2MnGa are calculated. We find that, in general, the bulk modulus increases with increasing e/a ratio (i.e., the number of valence electrons per atom). The shear moduli C' and C_{44} change oppositely with e/a ratio: C' decreases but C_{44} increases with increasing e/a. However, the Mn-rich Ga-deficient alloys deviate significantly from this general trend. The correlation of calculated elastic moduli and available experimental martensitic transformation temperatures (T_M) demonstrates that the alloy with larger C' than that of the perfect Ni_2MnGa generally possesses lower T_M except for $Ni_2Mn_{1+x}Ga_{1-x}$.

DOI: 10.1103/PhysRevB.79.144112 PACS number(s): 31.15.es, 75.50.Cc, 62.20.fg, 64.70.kd

I. INTRODUCTION

Ni_2MnGa alloy is an ideal candidate for actuator applications due to its magnetic shape memory effect induced by the reversible martensitic transformation (MT) between a high-temperature ferromagnetic $L2_1$ parent phase and a low-temperature tetragonal or orthorhombic martensitic phase. The combination of the magnetic and structural features results in its unique thermomagnetomechanical properties. For the standard stoichiometric Ni_2MnGa, the MT occurs at a temperature of 202 K (T_M), whereas the Curie temperature (T_C) is about 376 K.[1] Numerous experiments have shown that T_M is very sensitive to the composition of the alloy.[2–10] For examples, $Ni_{2.18}Mn_{0.82}Ga$ raises T_M to 340 K whereas the T_M of $Ni_{2.16}MnGa_{0.84}$ reaches 532 K.

Researchers have devoted themselves to exploring the physics underlying the composition dependent T_M of the Ni_2MnGa based alloys. There is a coarse-grained rule sug-

 ©2009 The American Physical Society

gested to relate the composition of the Ni_2MnGa based alloy to its T_M, i.e., a larger electron to atom ratio (e/a) corresponds to a higher T_M.[2,11] However, Sánchez-Alarcos *et al.*[12] have shown that both T_M and T_C depend on the quenching temperature and the subsequent heat treatment which changes the degree of the $L2_1$ long-range atomic order (site occupancy) of the alloy. This result demonstrated that site occupancy, beside the composition (e/a), can be a very important issue affecting the MT temperature of the Ni_2MnGa based alloys. On the other hand, the site occupancy in the off-stoichiometric Ni_2MnGa is critical to the modulated structure of the martensite.[13,14] Therefore, fundamental knowledge of the site occupancy is essential to the understanding of the MT behavior and thermomagnetomechanical properties of the Ni_2MnGa based alloys. For an off-stoichiometric Ni_2MnGa alloy at its thermal equilibrium state, the site occupancy seems to be straightforward, i.e., the excess atoms of the rich component simply occupy the sublattice(s) of the deficient one(s) (we define this scenario as the "normal" site occupation). For example, in $Ni_{2.18}Mn_{0.82}Ga$ alloy, one would expect that, if not considering the existence of vacancies, the excess Ni atoms take the Mn sublattice to form Ni antisite defects. This is probably why there has not been much attention paid on the determination of the site occupancy of off-stoichiometric Ni_2MnGa alloys so far. However, such an intuition may not be always correct. In the above example, we actually cannot rule out the possibility that the excess Ni atoms take the Ga sublattice (Ni antisite on Ga sublattice); in the meantime, some of the Ga atoms move to the Mn sublattice so as to introduce further Ga antisite on the Mn sublattice. In this case, the excess atoms of the rich component occupy the sublattice of the component at standard composition instead of the sublattice of the component in deficiency (we call this situation the "abnormal" site occupation). A very similar situation occurs in $TiNi_{1-x}Zr_x$ system, where we found that Zr atoms do not simply take the deficient Ni sublattice but prefer the Ti one and expel some Ti atoms to the Ni one.[15]

The MT of Ni_2MnGa alloy results from the soft-phonon modes and the soft shear modulus $C'=\frac{1}{2}(C_{11}-C_{12})$ of the high-temperature parent phase. For those alloys undergoing MT, it has long been realized (e.g., Refs. 16–20) that T_M is closely related to the single-crystal elastic modulus: the softer is the shear modulus (mainly C'), the higher the T_M. Such a model provides a possibility of determining the composition dependent T_M by surveying the composition dependent elastic modulus of the alloys. The model works reasonably well for the TiNi based shape memory alloys.[15,21,22] Since the elastic modulus is related not only to the composition but also to the site occupancy, one may expect that the elastic modulus might be a more suitable index for the composition dependent T_M than the e/a ratio for Ni_2MnGa based alloys. The elastic moduli of two off-stoichiometric Ni_2MnGa alloys have been measured by Stipcich *et al.*[23] Unfortunately, for most off-stoichiometric Ni_2MnGa alloys, the elastic modulus remains unknown. Therefore, the connection between the composition dependent elastic modulus and T_M for this particular alloy needs to be confirmed.

The purpose of the paper is to determine first the site occupancy of off-stoichiometric Ni_2MnGa alloys by the use of a first-principles method. Based on the determined site occupancy, the elastic moduli of the alloys are calculated. The connection between the composition dependent elastic modulus and available experimental T_M is discussed. The paper is arranged as follows: in Sec. II, we describe the first-principles method we used and the calculation details; in Sec. III, the properties of the standard stoichiometric Ni_2MnGa are presented in comparison with available theoretical and experimental data; the site occupancies of nine types of off-stoichiometric Ni_2MnGa alloys are reported in Sec. IV; in Sec. V, we present the calculated elastic modulus. The connection between the elastic modulus and T_M is discussed in Sec. VI. Finally, we summarize the main results of this work in Sec. VII.

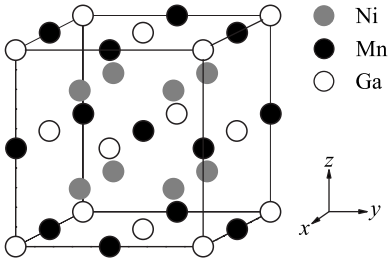

FIG. 1. Geometric structure of $L2_1$-Ni_2MnGa.

II. METHODS AND CALCULATION DETAILS

The first-principles method used in the present work is based on the density-functional theory (DFT).[24] The one-electron Kohn-Sham equation is solved by the use of a Green's function technique. The Green's function was calculated for 16 complex energy points distributed exponentially on a semicircular contour. The effective potential in the one-electron equation is treated with optimized overlapping muffin-tin approximation but the total energy is corrected with the so-called full charge-density (FCD) method.[25] In the one-center expansion of the full charge density, the number of orbitals we used is ten. The scalar-relativistic and frozen-core approximations are adopted. The Ni-$3d^8 4s^2$, Mn-$3d^5 4s^2$, and Ga-$3d^{10} 4s^2 4p^1$ are treated as valence states. The wave function is expanded using a basis sets of exact muffin-tin orbitals (EMTO).[25,26] The s, p, and d orbitals are included in the EMTO basis sets. The electronic exchange-correlation potential is described with the generalized-gradient approximation (GGA) parametrized by Perdew *et al.*[27] If not specified explicitly, the calculations are spin polarized since $L2_1$-Ni_2MnGa is ferromagnetic. The Brillouin zone is sampled by a uniform k-point mesh without using any smearing technique. The convergence of the elastic modulus with respect to the k-point mesh has been carefully tested for stoichiometric Ni_2MnGa, and finally we choose a k-point mesh of $17\times17\times17$ throughout our calculations.

For the stoichiometric Ni_2MnGa with cubic $L2_1$ structure, Ni atoms locate at the $(\frac{1}{4},\frac{1}{4},\frac{1}{4})$ and $(\frac{3}{4},\frac{3}{4},\frac{3}{4})$ sublattices, Mn atoms occupy the $(\frac{1}{2},\frac{1}{2},\frac{1}{2})$ sublattice, and Ga atoms occupy the (0,0,0) sublattice as shown in Fig. 1. For the off-stoichiometric Ni_2MnGa, if a sublattice is occupied by dif-

ferent atomic species, we assume that these atoms distribute randomly on the sublattice. The random distribution of these atoms is taken into account using the coherent-potential approximation (CPA).[28–30]

The stable site occupancy is determined by comparing the free energies per atom of the alloy with different site occupations. Taking into account the chemical mixing entropy, the free energy is expressed as

$$F = E + \frac{1}{4}k_B T \sum_{i=1}^{4} [x_i \ln x_i + (1-x_i)\ln(1-x_i)], \qquad (1)$$

where E is the electronic energy per atom calculated by the use of EMTO-CPA, x_i is the composition at each of the four sublattices, k_B is the Boltzmann constant, and T is the temperature. In the above equation, the lattice vibration and electronic temperature effects are neglected. At ambient condition, the electronic temperature effect is negligible. The contribution from lattice vibration to the free-energy difference (ΔF^{ph}) for alloys with different site-occupation configurations can be estimated approximately from the high-temperature expansion of the phonon free energy $\Delta F^{\mathrm{ph}} \approx 3k_B T(\Delta\Theta/\Theta)$ (Ref. 31). In the simplest approximation, the Debye temperatures (Θ) are proportional to $\sqrt{rB}$, where r is the Weigner-Seitz radius and B is the bulk modulus.[32] The changes in the bulk modulus and equilibrium lattice constant for different site occupancies are small. For example, the bulk modulus of $Ni_2Mn_{1-x}Ga_{1+x}$ drops from 151.3 GPa for the normal site-occupation configuration to 149.5 GPa for the abnormal one, whereas the Weigner-Seitz radius increases from 2.741 43 to 2.743 95 a.u., giving $\Delta\Theta/\Theta$ of about 0.0056. Therefore, the contribution from lattice vibration to the free-energy difference is typically two orders of magnitude smaller than that from electronic energy so that it is also negligible.

To calculate the elastic constants, we first determine the bulk modulus by fitting the calculated total energies versus volume to a Morse function.[33] Then the elastic moduli C' and C_{44} are calculated by the use of volume conserving orthorhombic and monoclinic deformations, i.e.,

$$\begin{pmatrix} 1+\epsilon_o & 0 & 0 \\ 0 & 1-\epsilon_o & 0 \\ 0 & 0 & \dfrac{1}{1-\epsilon_o^2} \end{pmatrix}, \qquad (2)$$

and

$$\begin{pmatrix} 1 & \epsilon_m & 0 \\ \epsilon_m & 1 & 0 \\ 0 & 0 & \dfrac{1}{1-\epsilon_m^2} \end{pmatrix}, \qquad (3)$$

respectively. Six strains $\epsilon = 0, 0.01, 0.02, \ldots, 0.05$ were used to calculate the total energies $E(\epsilon_o)$ and $E(\epsilon_m)$. The elastic constants C' and C_{44} are obtained by fitting the total energies with respect to ϵ_o and ϵ_m as $E(\epsilon_o) = E(0) + 2VC'\epsilon_o^2$ and $E(\epsilon_m) = E(0) + 2VC_{44}\epsilon_m^2$, respectively. C_{11} and C_{12} are then evaluated from the bulk modulus $B = \frac{1}{3}(C_{11} + 2C_{12})$ and the tetragonal shear constant $C' = \frac{1}{2}(C_{11} - C_{12})$.

TABLE I. Equilibrium lattice constant a, elastic constants C, bulk modulus B, and magnetic moment of $L2_1$-Ni_2MnGa. The data in the brackets are from soft-core calculations. The experimental elastic constants were measured at room temperature.

Parameter	This work	PP[a]	FLAPW[b]	Experiments
a (Å)	5.8922(5.8472)	5.8368	5.8104	5.8250[c]
B (GPa)	151.9(151.4)	155	156	146[d], 106[e]
C' (GPa)	15.9	2.5		4.5[d], 22[e]
C_{11} (GPa)	173.0	153		152[d], 136[e]
C_{12} (GPa)	141.3	148		143[d], 92[e]
C_{44} (GPa)	99.4	100		103[d], 102[e]
$\mu_0(\mu_B)$	4.05	4.27	4.09	4.17[c]
$\mu_{\mathrm{Ni}}(\mu_B)$	0.29		0.37	<0.3 [c]
$\mu_{\mathrm{Mn}}(\mu_B)$	3.54		3.36	3.86[c]
$\mu_{\mathrm{Ga}}(\mu_B)$	−0.07		−0.04	

[a]Reference 34.
[b]Reference 35.
[c]Reference 1.
[d]Reference 36.
[e]Reference 37.

III. PROPERTIES OF STANDARD STOICHIOMETRIC Ni_2MnGa

Listed in Table I are the equilibrium lattice constant, elastic constants, bulk modulus, and magnetic moment of perfect $L2_1$-Ni_2MnGa, in comparison with available experimental and other theoretical values reported in literature.

Our lattice constant (5.8922 Å) is larger than those from experiment (about 1%) as well as from the first-principles plane-wave pseudopotential and full-potential linearized augmented plane-wave (FLAPW) calculations, which is mainly due to the frozen-core approximation and a relatively small basis set adopted in the present calculations. If the soft-core approximation is used, the calculated lattice constant turns out to be 5.8472 Å. Increasing the orbital components in the EMTO basis set to s, p, d, and f further reduces the lattice constant to 5.8127 Å, in even better agreement with the experimental value (5.8250 Å). However, we consider that 1% overestimation of lattice constant is acceptable for first-principles calculations and, therefore, we use the frozen-core approximation, and s, p, and d basis set throughout this work in order to reduce the computational load.

The bulk modulus from our calculations is in good agreement with those from other first-principles calculations and experiments. Our test calculations demonstrated that the soft-core approximation yields a bulk modulus (151.4 GPa) almost the same as the frozen-core approximation does. The shear modulus C_{44} from different theoretical calculations is in good agreement with the experimental values. C' is the shear modulus that is critical to the MT of Ni_2MnGa. The experimental room temperature C' is scattered from 4.5 to 22 GPa. Our theoretical value evaluated at zero temperature

TABLE II. Relative electronic energy (in mRy), ΔE and $\Delta E'$, and free energy (ΔF) of the off-stoichiometric $L2_1$-Ni_2MnGa to that of the alloy with normal site occupancy configuration, at temperature of 300 K. $\Delta E'$ is the relative electronic energy from nonspin-polarized calculations with the spin-polarized equilibrium lattice constants. Also presented in the table are the magnetic moments μ_0 (in μ_B).

Type	Composition	Site occupancy	ΔE	ΔF	μ_0	$\Delta E'$
1	$Ni_{2+2x}Mn_{1-x}Ga_{1-x}$ (x=0.05)	$Ni_2(Mn_{0.95}Ni_{0.05})(Ga_{0.95}Ni_{0.05})$	0	0	3.91	0
		$Ni_2(Mn_{0.95}Ga_{0.05})(Ga_{0.90}Ni_{0.10})$	0.12	0.06	3.92	0.01
		$Ni_2(Mn_{0.90}Ni_{0.10})(Ga_{0.95}Mn_{0.05})$	0.32	0.26	3.92	−0.26
	$Ni_{2+2x}Mn_{1-x}Ga_{1-x}$ (x=0.10)	$Ni_2(Mn_{0.90}Ni_{0.10})(Ga_{0.90}Ni_{0.10})$	0	0	3.76	0
		$Ni_2(Mn_{0.80}Ni_{0.20})(Ga_{0.90}Mn_{0.10})$	0.67	0.59	3.80	−0.50
2	$Ni_{2-2x}Mn_{1+3x}Ga_{1-x}$ (x=0.05)	$(Ni_{1.90}Mn_{0.10})Mn(Ga_{0.95}Mn_{0.05})$	0	0	3.49	0
		$(Ni_{1.85}Mn_{0.15})Mn(Ga_{0.95}Ni_{0.05})$	0.28	0.22	3.54	−0.59
		$(Ni_{1.90}Ga_{0.10})Mn(Ga_{0.85}Mn_{0.15})$	1.67	1.56	3.41	2.71
	$Ni_{2-2x}Mn_{1+3x}Ga_{1-x}$ (x=0.10)	$(Ni_{1.80}Mn_{0.20})Mn(Ga_{0.90}Mn_{0.10})$	0	0	2.97	0
		$(Ni_{1.70}Mn_{0.30})Mn(Ga_{0.90}Ni_{0.10})$	0.42	0.33	3.04	−1.07
		$(Ni_{1.80}Ga_{0.20})Mn(Ga_{0.70}Mn_{0.30})$	2.59	2.46	2.85	5.14
3	$Ni_{2-2x}Mn_{1-x}Ga_{1+3x}$ (x=0.05)	$(Ni_{1.90}Ga_{0.10})(Mn_{0.95}Ga_{0.05})Ga$	0	0	3.82	0
		$(Ni_{1.90}Mn_{0.10})(Mn_{0.85}Ga_{0.15})Ga$	−0.67	−0.78	3.12	−3.25
		$(Ni_{1.85}Ga_{0.15})(Mn_{0.95}Ni_{0.05})Ga$	0.93	0.87	3.81	0.63
	$Ni_{2-2x}Mn_{1-x}Ga_{1+3x}$ (x=0.10)	$(Ni_{1.80}Ga_{0.20})(Mn_{0.90}Ga_{0.10})Ga$	0	0	3.58	0
		$(Ni_{1.80}Mn_{0.20})(Mn_{0.70}Ga_{0.30})Ga$	−1.53	−1.66	2.22	−6.53
		$(Ni_{1.70}Ga_{0.30})(Mn_{0.90}Ni_{0.10})Ga$	1.69	1.60	3.56	1.08
4	$Ni_{2+x}MnGa_{1-x}$ (x=0.10)	$Ni_2Mn(Ga_{0.90}Ni_{0.10})$	0	0	4.13	0
		$Ni_2(Mn_{0.90}Ni_{0.10})(Ga_{0.90}Mn_{0.10})$	0.65	0.49	4.17	−0.52
5	$Ni_{2+x}Mn_{1-x}Ga$ (x=0.10)	$Ni_2(Mn_{0.90}Ni_{0.10})Ga$	0	0	3.69	0
		$Ni_2(Mn_{0.90}Ga_{0.10})(Ga_{0.90}Ni_{0.10})$	0.59	0.44	3.69	0.05
6	$Ni_{2-x}MnGa_{1+x}$ (x=0.10)	$(Ni_{1.90}Ga_{0.10})MnGa$	0	0	4.02	0
		$(Ni_{1.90}Mn_{0.10})(Mn_{0.90}Ga_{0.10})Ga$	−0.62	−0.77	3.32	−3.02
7	$Ni_{2-x}Mn_{1+x}Ga$ (x=0.10)	$(Ni_{1.90}Mn_{0.10})MnGa$	0	0	3.69	0
		$(Ni_{1.90}Ga_{0.10})Mn(Ga_{0.90}Mn_{0.10})$	1.86	1.71	3.61	2.70
8	$Ni_2Mn_{1+x}Ga_{1-x}$ (x=0.10)	$Ni_2Mn(Ga_{0.90}Mn_{0.10})$	0	0	4.51	0
		$(Ni_{1.90}Mn_{0.10})Mn(Ga_{0.90}Ni_{0.10})$	0.59	0.40	3.75	−1.28
9	$Ni_2Mn_{1-x}Ga_{1+x}$ (x=0.10)	$Ni_2(Mn_{0.90}Ga_{0.10})Ga$	0	0	3.63	0
		$(Ni_{1.90}Ga_{0.10})(Mn_{0.90}Ni_{0.10})Ga$	1.96	1.78	3.65	1.44

falls into this range but is significantly larger than that from the plane-wave pseudopotential calculation. Raising temperature may change the elastic modulus. Nevertheless, it should be noted that the main purpose of this work is to survey the composition dependence of the elastic moduli. The relative elastic modulus of the off-stoichiometric Ni_2MnGa alloys to that of the stoichiometric one is expected to be less dependent on temperature.

Theoretical magnetic moments from various methods are in reasonably good agreement with experimental data. The error bar is less than $\pm 3\%$. The magnetic moment is mainly localized on the Mn sublattice. Our calculation yields a total magnetic moment in line with the FLAPW calculation, which is slightly smaller than the experimental value, whereas the magnetic moment from the plane-wave pseudopotential calculation is slightly larger than that from experiment.

IV. SITE OCCUPANCY AND MAGNETIC MOMENTS OF OFF-STOICHIOMETRIC Ni_2MnGa

In the present work, we consider nine types of off-stoichiometric Ni_2MnGa alloys with 12 different compositions. In principle, the off stoichiometry can be achieved by the formation of antisite defects and/or vacancies. However, our previous calculations using the projector augmented wave method with a general gradient approximation have demonstrated that the vacancy formation energies in Ni_2MnGa are much higher than the formation energies of various antisite defects.[38] Therefore, in this work, the formation of vacancies in the alloys is not considered.

Listed in Table II are the electronic energy (E) and free energy (F) of the off-stoichiometric Ni_2MnGa of different site occupations relative to that with the normal site occupation. Positive ΔF means that the normal site-occupation con-

figuration is lower in energy and, therefore, is more stable than the abnormal one.

Since the energy difference between different site occupations of an off-stoichiometric alloy is quite small, we choose two compositions for the $Ni_{2+2x}Mn_{1-x}Ga_{1-x}$ (type 1), $Ni_{2-2x}Mn_{1+3x}Ga_{1-x}$ (type 2), and $Ni_{2-2x}Mn_{1-x}Ga_{1+3x}$ (type 3) alloys in order to check the reliability of our calculations. It is shown that the stability sequences for these alloys do not change with different compositions ($x=0.05,0.10$), indicating that the relative stability of the site occupations determined in this work is reasonable.

The difference between ΔE and ΔF for an alloy with the same site-occupation configuration is very small at the temperature of 300 K. Therefore, in the temperature range of interest, the mixing entropy cannot change the relative stability of the site occupations such that comparing the electronic energy is actually sufficient to determine the stable site occupancy.

As is shown in Table II, the normal site occupation for most of the off-stoichiometric alloys is more stable than the abnormal one. However, this is not the case for $Ni_{2-2x}Mn_{1-x}Ga_{1+3x}$ (type 3) and $Ni_{2-x}MnGa_{1+x}$ ($x=0.10$, type 6). In the $Ni_{2-2x}Mn_{1-x}Ga_{1+3x}$ alloy, the excess Ga atoms do not occupy evenly the two Ni sublattices and the Mn sublattice but occupy solely the Mn sublattice whereas some of the Mn atoms move to the Ni sublattices. Similarly, in the $Ni_{2-x}MnGa_{1+x}$ ($x=0.10$) alloy, the excess Ga atoms again prefer the Mn sublattice although it is Ni instead of Mn that is in deficiency.

The site occupancy in off-stoichiometric Ni_2MnGa alloy has rarely been addressed in literature. Most recently, the site occupancy of $Ni_2Mn_{1+x}Ga_{1-x}$ has been determined by Sánchez-Alarcos *et al.*,[12] which shows that the excess Mn atoms occupy the Ga sublattice, in line with our theoretical prediction.

Listed also in Table II are the magnetic moments of the off-stoichiometric Ni_2MnGa alloys with different site occupations. Examining the local magnetic moments on each sublattices (not shown in the table), we find that a Mn atom changes its magnetic moment when occupying different sublattices: for all the off-stoichiometric alloys involved in this work, the magnetic moments of a Mn atom on the Mn, Ni, and Ga sublattices are roughly $3.5\mu_B$, $-2.5\mu_B$, and $\pm 3.2\mu_B$, respectively. + or − means that the atom can be ferromagnetic or antiferromagnetic coupling with that of the Mn atoms on the Mn sublattice, depending on the composition of the alloy. Observing the geometric structure of the $L2_1$-Ni_2MnGa (see Fig. 1), it is clear that nearest neighboring Mn atoms, locating, respectively, at Mn and Ni sublattices, prefer to have magnetic moments with opposite orientations. When occupying the Mn sublattice, Ni and Ga atoms are also spin polarized with local magnetic moments of about $0.50\mu_B$ and $0.36\mu_B$, respectively, in comparison with about $0.29\mu_B$ and $-0.07\mu_B$ when they locate at their normal sublattices. The magnetic moments of a Ni atom on the Ga sublattice and a Ga atom on the Ni sublattice are negligible.

Since the atoms (mainly Mn) exhibit different magnetic moments when occupying different sublattices, the magnetic property of the alloy also changes with different site-occupation configurations. Obviously, the site occupancy of the off-stoichiometric Ni_2MnGa is controlled by the complex interaction between the chemical and magnetic effects. In Table II, we compared the relative electronic energies ΔE and $\Delta E'$ calculated, respectively, with and without spin polarization, which may roughly show the magnetic effect on the site occupancy. It is seen that, for the same alloy, if there exist Mn atoms occupying different sublattices in different site-occupation configurations, ΔE differs dramatically from $\Delta E'$, indicating that the magnetic effect on the site occupancy is very strong. For some of the alloys, the magnetic effect even alters the stability sequence of the site occupations. For example, the abnormal site occupation of $Ni_{2+x}MnGa_{1-x}$ ($x=0.10$, type 4) and $Ni_2Mn_{1+x}Ga_{1-x}$ ($x=0.10$, type 8) is more stable than the normal one from nonspin-polarized calculations but the latter becomes more stable from spin-polarized calculations. For the alloy in which there are no Mn atoms changing their sublattice in different site-occupation configurations (e.g., $Ni_2Mn_{1-x}Ga_{1+x}$, $x=0.10$, and $Ni_{2+x}Mn_{1-x}Ga$, $x=0.10$), the difference between ΔE and $\Delta E'$ is much smaller than that in the case discussed above. The magnetic effect is complicated and composition dependent. For most alloys involved in this study, ΔE is larger than $\Delta E'$, which means that the magnetic effect tends to stabilize the normal site-occupation configuration. However, for the $Ni_{2-x}Mn_{1+x}Ga$ ($x=0.10$) alloy, the magnetic effect stabilizes the abnormal site occupation.

V. ELASTIC MODULUS OF OFF-STOICHIOMETRIC Ni_2MnGa

With the site occupancy determined in Sec. IV, we calculate the elastic modulus of the off-stoichiometric Ni_2MnGa as listed in Table III. As shown in the table, Ga-rich alloys generally possess significantly high C' than that of the standard stoichiometric Ni_2MnGa. Excess Ni atoms decrease greatly C'. For the Mn-rich alloys, if both Ni and Ga are in deficiency, C' is lower than that of the perfect Ni_2MnGa. However, if either Ni or Ga is deficient in the Mn-rich alloys, C' remains almost unchanged.

Since both elastic modulus and e/a are believed to be related to the MT behavior of the shape memory Ni_2MnGa alloys, there should also be certain intrinsic connection between them. Figure 2 shows the relationship between the e/a ratio and the bulk as well as the shear moduli of the off-stoichiometric Ni_2MnGa alloys. We see that the general trend is that the bulk modulus increases with e/a. C' and C_{44} change oppositely with increasing e/a: C' decreases but C_{44} increases. The bulk modulus changes more significantly at the low e/a side than at the high e/a side but C' and C_{44} are the opposite. It is noted that there are three data points (the green open symbols in figure) heavily deviating from the general trend of the elastic modulus with respect to the e/a ratio. These three data points correspond to $Ni_{2-2x}Mn_{1+3x}Ga_{1-x}$ ($x=0.05,0.10$, type 2) and $Ni_2Mn_{1+x}Ga_{1-x}$ ($x=0.10$, type 8). We suggest that the deviation might be due to the magnetic interaction between the Mn atoms on the Ga sublattice and those on the Mn sublattice since all the three alloys have their excess Mn atoms located on the Ga sublattice. A direct confirmation of this

TABLE III. Lattice constant (in angstroms), elastic properties (in GPa), and e/a ratio of off-stoichiometric $L2_1$-Ni_2MnGa with stable site-occupation configuration.

Type	Composition	Lattice Constant	B	C'	C_{11}	C_{12}	C_{44}	e/a [a]
0	Ni_2MnGa	5.8922	151.9	15.9	173.0	141.6	99.4	7.500
1	$Ni_{2+2x}Mn_{1-x}Ga_{1-x}$ (x=0.05)	5.8808	153.5	12.5	170.2	145.1	101.9	7.625
	$Ni_{2+2x}Mn_{1-x}Ga_{1-x}$ (x=0.10)	5.8690	155.3	9.1	167.5	149.2	104.4	7.750
2	$Ni_{2-2x}Mn_{1+3x}Ga_{1-x}$ (x=0.05)	5.9035	146.1	14.5	165.3	136.4	97.4	7.475
	$Ni_{2-2x}Mn_{1+3x}Ga_{1-x}$ (x=0.10)	5.9107	148.6	13.2	166.2	139.8	95.4	7.450
3	$Ni_{2-2x}Mn_{1-x}Ga_{1+3x}$ (x=0.05)	5.9035	149.0	18.6	173.8	136.6	94.9	7.275
	$Ni_{2-2x}Mn_{1-x}Ga_{1+3x}$ (x=0.10)	5.9054	140.8	20.0	167.5	127.4	92.2	7.050
4	$Ni_{2+x}MnGa_{1-x}$ (x=0.10)	5.8809	153.4	11.4	168.5	145.8	103.2	7.675
5	$Ni_{2+x}Mn_{1-x}Ga$ (x=0.10)	5.8808	153.6	13.4	171.4	144.7	100.7	7.575
6	$Ni_{2-x}MnGa_{1+x}$ (x=0.10)	5.9106	150.6	17.6	174.1	138.8	94.8	7.325
7	$Ni_{2-x}Mn_{1+x}Ga$ (x=0.10)	5.8997	151.7	16.1	173.1	141.0	99.3	7.425
8	$Ni_2Mn_{1+x}Ga_{1-x}$ (x=0.10)	5.8977	148.6	16.0	169.9	137.9	99.6	7.600
9	$Ni_2Mn_{1-x}Ga_{1+x}$ (x=0.10)	5.8927	151.3	18.1	175.5	139.3	96.9	7.400

[a]The Ga 3d electrons are quite deep in energy and contribute little to the cohesion of the system. Therefore, in accordance with the e/a ratio of Ni_2MnGa based alloys defined in literature, here, the Ga 3d electrons are not counted as valence electrons although we treat them as valence electrons in our calculations.

point is a difficult task. However, we note that the deviation disappears if performing nonspin-polarized calculations. From spin-polarization calculations, with e/a increasing from 7.325 for $Ni_{2-x}MnGa_{1+x}$ (x=0.10) to 7.500 for Ni_2MnGa, the bulk modulus increases from 150.6 to 151.9 GPa but it drops to 148.6 GPa for $Ni_2Mn_{1+x}Ga_{1-x}$ (x=0.10) with e/a further increasing to 7.600. Here, $Ni_2Mn_{1+x}Ga_{1-x}$ (x=0.10) is the alloy whose bulk modulus deviates from the general monotonous $B-e/a$ trend. From nonspin-polarized calculations, the bulk modulus increases monotonously from 184.5 to 186.3 to 190.0 GPa for $Ni_{2-x}MnGa_{1+x}$ (x=0.10), Ni_2MnGa, and $Ni_2Mn_{1+x}Ga_{1-x}$ (x=0.10), respectively, with increasing e/a ratio. The above results demonstrate that magnetic interaction indeed plays an important role in influencing the $B-e/a$ relationship. Hopefully, this may serve as an indirect evidence in support to our suggestion.

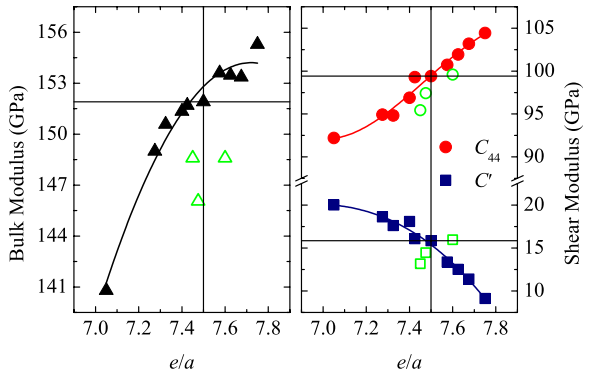

FIG. 2. (Color online) Bulk (left panel) and shear (right panel) moduli of off-stoichiometric Ni_2MnGa alloys with respect to e/a ratio. The vertical and horizontal lines within the figures refer to the elastic moduli and e/a ratio of the standard stoichiometric Ni_2MnGa. The fitting curves are to guide the view.

VI. CORRELATION BETWEEN C' AND T_M

In order to get an idea of the connection between the composition dependent elastic modulus and the T_M of Ni_2MnGa alloy, in Table IV, we collect the experimental T_M of some off-stoichiometric Ni_2MnGa alloys. These alloys match roughly the nine types of off-stoichiometric Ni_2MnGa although their compositions may not be exactly the same as those studied in the present work. Figure 3 shows the experimental T_M with respect to C' and e/a ratio of the alloys. C' of the alloys with compositions not included in the present calculations are obtained through linear interpolation or extrapolation from the calculated ones. As shown in the right panel of Fig. 3, T_M goes up with increasing e/a ratio as it is noted previously in literature.[2,11] From the left panel of Fig. 3, we see that the alloy of larger C' generally possesses

TABLE IV. Collection of experimental martensitic transformation temperature of off-stoichiometric Ni_2MnGa.

Type	Composition	T_M	Source
0	Ni_2MnGa	202	Ref. 1
	$Ni_{2.104}Mn_{0.940}Ga_{0.956}$	278	Ref. 2
1	$Ni_{2.160}Mn_{0.936}Ga_{0.904}$	340	Ref. 3
2	$Ni_{1.908}Mn_{1.220}Ga_{0.872}$	227	Ref. 2
3	$Ni_{1.988}Mn_{0.972}Ga_{1.040}$	184	Ref. 2
4	$Ni_{2.16}MnGa_{0.84}$	532	Ref. 4
5	$Ni_{2+x}Mn_{1-x}Ga$ ($0.02<x<0.20$)	220–340	Refs. 5–7
6	Ni-deficient, Ga-rich	not found	
7	Ni-deficient, Mn-rich	not found	
	$Ni_2Mn_{1.20}Ga_{0.80}$	360	Ref. 8
8	$Ni_2Mn_{1.05}Ga_{0.95}$	220	Ref. 10
9	$Ni_{1.984}Mn_{0.876}Ga_{1.14}$	<4.2	Ref. 2

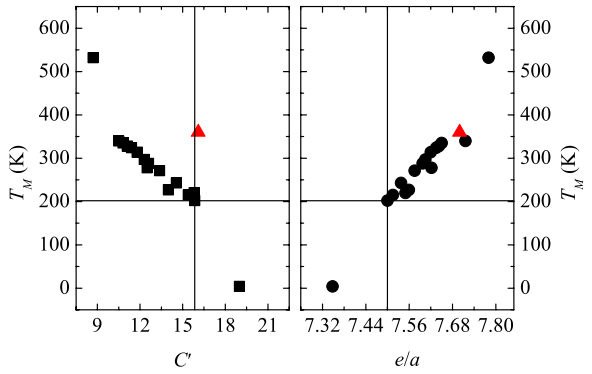

FIG. 3. (Color online) Experimental martensitic transformation temperature (T_M) with respect to the shear modulus C' (left panel) and e/a ratio (right panel) of the off-stoichiometric Ni_2MnGa alloys. The vertical lines within the figures refer to the C' and e/a ratio, and the horizontal lines refer to the T_M of the standard stoichiometric Ni_2MnGa.

lower T_M except for $Ni_2Mn_{1+x}Ga_{1-x}$ ($x=0.20$, the red triangle in Fig. 3). C' of $Ni_2Mn_{1+x}Ga_{1-x}$ ($x=0.20$) is almost the same as Ni_2MnGa. However, the experimental T_M of the alloy is higher than that of perfect Ni_2MnGa. The higher T_M of $Ni_2Mn_{1+x}Ga_{1-x}$ ($x=0.20$) is in agreement with its larger e/a ratio (see Table III). From this point of view, e/a ratio seems to be a better index for the composition dependent T_M. However, for the alloys with the same composition but with different long-range atomic order (site occupancy) corresponding to different heat treatment history, C' could be a better index since, in this case, the e/a ratio is exactly the same but C' changes. Our work addressing this topic is now ongoing, and we are checking the relationship between the elastic modulus and long-range-order parameter of the Ni_2MnGa based alloy with a specific composition.

VII. SUMMARY

In this paper, the site occupancy and elastic constants of off-stoichiometric Ni_2MnGa are investigated by the use of a first-principles EMTO-CPA method. The main results are summarized as follows:

(1) For most of the off-stoichiometric Ni_2MnGa, the normal site occupation is favorable, i.e., the excess atoms of the rich component occupy the sublattice(s) of the deficient component(s). Nevertheless, for the Ga-rich alloys, the excess Ga atoms always prefer to take the Mn sublattice no matter if Mn is deficient or not.

(2) In general, the bulk modulus increases with increasing e/a ratio. The shear moduli C' and C_{44} change oppositely with e/a ratio: C' decreases but C_{44} increases with increasing e/a. However, the Mn-rich Ga-deficient alloys deviate significantly from this general trend.

(3) An examination of the calculated elastic modulus and available experimental martensitic transformation temperature (T_M) demonstrates that the alloy with a larger C' generally possesses a lower T_M except for $Ni_2Mn_{1+x}Ga_{1-x}$.

ACKNOWLEDGMENTS

The authors acknowledge the financial support from the MoST of China under Grant No. 2006CB605104, from the NSFC under Grants No. 50631030, No. 50871114, and No. 08-02-92201a (RFBR-NSFC project for the Sino-Russian cooperation). The Swedish Research Council, the Swedish Foundation for Strategic Research, the Hungarian Scientific Research Fund (Contract No. T048827), and the Carl Tryggers Foundation are also acknowledged for financial support.

*Corresponding author; qmhu@imr.ac.cn

[1] P. J. Webster, K. R. A. Ziebeck, S. L. Town, and M. S. Peak, Philos. Mag. B **49**, 295 (1984).
[2] V. A. Chernenko, J. Pons, C. Segui, and E. Cesari, Acta Mater. **50**, 53 (2002).
[3] M. Ohtsuka, M. Matsumoto, and K. Itagaki, Mater. Sci. Eng., A **438-440**, 935 (2006).
[4] Y. Li, Y. Xin, C. Jiang, and H. Xu, Mater. Sci. Eng., A **438-440**, 978 (2006).
[5] K. Inoue, Y. Yamaguichi, K. Ohsumi, Y. Noda, H. Kimura, K. Kusaka, and T. Nakagawa, Mater. Sci. Eng., A **438-440**, 131 (2006).
[6] A. N. Vasil'ev, A. D. Bozhko, V. V. Khovailo, I. E. Dikshtein, V. G. Shavrov, V. D. Buchelnikov, M. Matsumoto, S. Suzuki, T. Takagi, and J. Tani, Phys. Rev. B **59**, 1113 (1999).
[7] V. V. Khovailo, T. Takagi, A. D. Bozhko, M. Matsumoto, J. Tani, and V. G. Shavrov, J. Phys.: Condens. Matter **13**, 9655 (2001).
[8] F. Albertini, A. Paoluzi, L. Pareti, M. Solzi, L. Righi, E. Villa, S. Besseghini, and F. Passaretti, J. Appl. Phys. **100**, 023908 (2006).
[9] G. H. Wu, C. H. Yu, L. Q. Meng, J. L. Chen, F. M. Yang, S. R. Qi, W. S. Zhan, Z. Wang, Y. F. Zheng, and L. C. Zhao, Appl. Phys. Lett. **75**, 2990 (1999).
[10] R. Ranjan, S. Banik, S. R. Barman, U. Kumar, P. K. Mukhopadhyay, and D. Pandey, Phys. Rev. B **74**, 224443 (2006).
[11] A. T. Zayak, W. A. Adeagbo, P. Entel, and K. M. Rabe, Appl. Phys. Lett. **88**, 111903 (2006).
[12] V. Sánchez-Alarcos, V. Recarte, J. I. Pérez-Landazábal, and G. J. Cuello, Acta Mater. **55**, 3883 (2007).
[13] A. T. Zayak and P. Entel, Mater. Sci. Eng., A **378**, 419 (2004).
[14] M. Gigla, P. Szczeszek, and H. Morawiec, Mater. Sci. Eng., A **438-440**, 1015 (2006).
[15] Q. M. Hu, R. Yang, J. M. Lu, L. Wang, B. Johansson, and L. Vitos, Phys. Rev. B **76**, 224201 (2007).
[16] F. Falk, Acta Metall. **28**, 1773 (1980); F. Falk and P. Konopka, J. Phys.: Condens. Matter **2**, 61 (1990).
[17] O. Nittono and Y. Koyama, Jpn. J. Appl. Phys. **21**, 680 (1982); Y. Koyama and O. Nittono, J. Phys. Colloq. **43**, C4 145 (1982).
[18] J. K. Liakos and G. A. Saunders, Philos. Mag. A **46**, 217 (1982).
[19] G. R. Barsch and J. A. Krumhansl, Phys. Rev. Lett. **53**, 1069 (1984).
[20] X. Ren and K. Otsuka, Mater. Sci. Forum **327-328**, 429 (2000); X. Ren, K. Otsuka, and T. Suzuki, J. Alloys Compd. **355**, 196 (2003); K. Otsuka and X. Ren, Prog. Mater. Sci. **50**, 511 (2005).

[21] J. M. Lu, Q. M. Hu, and R. Yang, Acta Mater. **56**, 4913 (2008).
[22] J. M. Lu, Q. M. Hu, and R. Yang, in *Advanced Intermetallic-based Alloys for Extreme Environment and Energy Applications*, edited by B. Bewley, Y. He, M. Palm, M. Takeyama, and J. Wiezorek, MRS Symposia Proceedings (to be published).
[23] M. Stipcich, L. Mañosa, Antoni Planes, M. Morin, J. Zarestky, T. Lograsso, and C. Stassis, Phys. Rev. B **70**, 054115 (2004).
[24] R. M. Dreizler and E. K. U. Gross, *Density Functional Theory* (Pringer, Berlin, 1998).
[25] L. Vitos, in *Computational Quantum Mechanics for Materials Engineers* (Springer-Verlag, London, 2007).
[26] L. Vitos, Phys. Rev. B **64**, 014107 (2001).
[27] J. P. Perdew, K. Burke, and M. Ernzerhof, Phys. Rev. Lett. **77**, 3865 (1996).
[28] P. Soven, Phys. Rev. **156**, 809 (1967).
[29] B. L. Györffy, Phys. Rev. B **5**, 2382 (1972).
[30] L. Vitos, I. A. Abrikosov, and B. Johansson, Phys. Rev. Lett. **87**, 156401 (2001).
[31] G. Grimvall, Phys. Scr. **13**, 59 (1976).
[32] Per Söderlind and Börje Johansson, Thermochim. Acta **218**, 145 (1993).
[33] V. L. Moruzzi, J. F. Janak, and K. Schwarz, Phys. Rev. B **37**, 790 (1988).
[34] C. Bungaro, K. M. Rabe, and A. Dal Corso, Phys. Rev. B **68**, 134104 (2003).
[35] A. Ayuela, J. Enkovaara, K. Ullakko, and R. M. Nieminen, J. Phys.: Condens. Matter **11**, 2017 (1999).
[36] J. Worgull, E. Petti, and J. Trivisonno, Phys. Rev. B **54**, 15695 (1996).
[37] L. Manosa, A. Gonzalez-Comas, E. Obrado, A. Planes, V. A. Chernenko, V. V. Kokorin, and E. Cesari, Phys. Rev. B **55**, 11068 (1997).
[38] Our previous calculations using the projector augmented wave method with a general gradient approximation yielded 0.61 and 0.32 eV for the formation energies of Mn antisite on Ni sublattice and Ni antisite on Mn sublattice, respectively. The formation energies of the vacancies on Ni, Mn, and Ga sublattices are 1.04, 1.23, and 3.10 eV, respectively.